Using Electronic Polarization From the Internal Continuum (EPIC) for Intermolecular Interactions

JEAN-FRANÇOIS TRUCHON,[1,2] ANTHONY NICHOLL'S,[3] J. ANDREW GRANT,[4] RADU I. IFTIMIE,[1] BENOÎT ROUX,[5] CHRISTOPHER I. BAYLY[2]

[1]*Département de chimie, Université de Montréal, C.P. 6128 Succursale centre-ville, Montréal, Québec, Canada H3C 3J7*
[2]*Merck Frosst Canada Ltd., 16711 TransCanada Highway, Kirkland, Québec, Canada H9H 3L1*
[3]*OpenEye Scientific Software, Inc., Santa Fe, New Mexico 87508*
[4]*AstraZeneca Pharmaceuticals Mereside, Macclesfield, Cheshire SK10 4TF, England*
[5]*Institute of Molecular Pediatric Sciences, Gordon Center for Integrative Science, University of Chicago, Illinois 929 East 57th Street, Chicago, Illinois 60637*

Abstract: Recently, the vacuum-phase molecular polarizability tensor of various molecules has been accurately modeled (Truchon et al., J Chem Theory Comput 2008, 4, 1480) with an intramolecular continuum dielectric model. This preliminary study showed that electronic polarization can be accurately modeled when combined with appropriate dielectric constants and atomic radii. In this article, using the parameters developed to reproduce *ab initio* quantum mechanical (QM) molecular polarizability tensors, we extend the application of the "electronic polarization from internal continuu" (EPIC) approach to intermolecular interactions. We first derive a dielectric-adapted least-square-fit procedure similar to RESP, called DRESP, to generate atomic partial charges based on a fit to a QM *ab initio* electrostatic potential (ESP). We also outline a procedure to adapt any existing charge model to EPIC. The ability of this to reproduce local polarization, as opposed to uniform polarization, is also examined leading to an induced ESP relative root mean square deviation of 1%, relative to *ab initio*, when averaged over 37 molecules including aromatics and alkanes. The advantage of using a continuum model as opposed to an atom-centered polarizable potential is illustrated with a symmetrically perturbed atom and benzene. We apply EPIC to a cation-π binding system formed by an atomic cation and benzene and show that the EPIC approach can accurately account for the induction energy. Finally, this article shows that the *ab initio* electrostatic component in the difficult case of the H-bonded 4-pyridone dimer, a highly polar and polarized interaction, is well reproduced without adjusting the vacuum-phase parameters.

© 2009 Wiley Periodicals, Inc.   J Comput Chem 31: 811–824, 2010

Key words: polarizable force field; Poisson-Boltzman; dielectric; RESP; electronic polarization

Introduction

An intramolecular continuum dielectric model has been recently applied to the calculation of molecular polarizabilities and shown to accurately reproduce those computed using high-level *ab intio* Quantum Mechanical (QM) calculations.[1] The electronic polarization from internal continuum (EPIC) approach showed that, relative to other methods, significantly fewer parameters were required to describe the anisotropy in molecular polarizability; this was illustrated by calculations on a set of aromatic, diatomic and alkane molecules. This work focuses on the ability of the parameterized EPIC model to reproduce electrostatic potentials (ESP) and in particular the response of this potential

to external electric fields typical of those responsible for electronic polarization in intermolecular interactions. This is considered an essential feature for force-field based methodologies.

Many researchers have published work on combining a polarizable force-field with Poisson-Boltzmann (PB) formalism

---

mainly to take advantage of the implicit solvent averaging modeled by a solvent dielectric constant. For example, the "polarizable force field" (PFF)[2] combines a point induced dipole (PID) model with a continuum solvent. Similarly the "atomic multipole optimized energetics for biomolecular applications" (AMOEBA) force field couples a static multipolar expansion with atomic polarizabilities[3] in the context of a PB description of solvent. However, such models are computationally complex requiring atomic tensors to model response effects. In contrast, this work demonstrates that solute polarizability can be modeled using simple dielectric response theory, and requires only a small number of fitted atomic radii and isotropic relative permittivities (dielectrics). Here, however, we focus on explicit interactions, not on solvent reaction fields. Complex electron distributions and response are modeled using simple atom-centered point charges combined with a continuum dielectric. A crucial feature of the model is that screening effects produced by intramolecular polarization of the dielectric are explicitly accounted for in calculating atomic charges by least-squares fitting to the ESP computed using *ab initio* QM techniques. This is in contrast to conventional ESP-fitting methods,[4–9] all of which are constructed around the assumptions that there is no dielectric boundary and that the internal dielectric is 1.

This article describes a new formalism, called DRESP, for calculating atomic charges from the QM ESP so as to accommodate a dielectric boundary with an internal dielectric greater than one. In the rest of this article, we derive the equations relative to DRESP and show the resulting charges on few examples. Additionally, we propose a general way of adapting an existing charge model to behave properly when used with EPIC and we show its performances in reproducing the AM1-BCC[10,11] permanent ESP on selected molecules. The ability of the proposed polarization model to reproduce the response to nonuniform perturbations is also examined. In doing this, we have found that it is not necessary to refit radii and dielectric values optimized based on the vacuum-phase molecular polarizabilities only, thus our previously published parameter sets[1] are directly applied. These findings suggest that a general small molecule polarizable model based on continuum electrostatics could be developed. Finally, we apply the EPIC polarizable model to two problems of fundamental importance in biological applications (namely cation-π binding and H-bonding) to demonstrate its performance.

Methods

Below, the new least-squares method, hereafter named DRESP, is derived for fitting atomic point charges to a QM ESP in the presence of an internal dielectric. The computational details for both the finite difference Poisson's equation (PE) solver and B3LYP calculations are then presented. Details on the calculation of the induced ESP are also given. Finally, the molecule dataset used to validate the current approaches is described.

A Least-Squares Method

The derivation presented in this section is a necessary recasting of the least-squares method already in use to fit atomic charges to an ESP computed on a grid. Conventional ESP-fitting methods are all formalized by using Coulomb's law with the assumption of a constant dielectric, in general 1. These formalisms could be trivially extended to constant dielectrics higher than 1, but only if the dielectric is uniform through all space. What makes the new formalism presented here necessary is that if the internal dielectric of a molecule is greater than 1, there is a critical dielectric boundary between that and the vacuum dielectric of 1 where the QM ESP is evaluated. As a result, the least-squares fitting problem requires Coulomb's law to be solved in the context of a varying dielectric between the inner dielectric (>1) and the outer vacuum dielectric of 1. The usual algebraic solution cannot apply; a different treatment is required. For example, Tan and Luo[12] designed an iterative optimization scheme. The objective here is to obtain a set of equations linear in the atomic charges that can be easily and quickly solved in a single pass computationally. The following derivation uses the linearity of Poisson's equation in both the charge density and the potential such that the solution for each individual charge can be superimposed to produce the correct solution for the entire system.

From a very general standpoint, the ESP $\varphi(\vec{r})$ at a point $\vec{r}$ in space can be calculated by solving the electrostatics-related Poisson's equation, given by eq. (1), with the appropriate boundary conditions

$$\vec{\nabla} \cdot (\varepsilon_0 \varepsilon(\vec{r}) \vec{\nabla} \varphi(\vec{r})) = -\rho(\vec{r}) \tag{1}$$

where $\varepsilon(\vec{r})$ is the system dielectric function, ε_0 is the vacuum permittivity and $\rho(\vec{r})$ the charge density function. In the case where $\varepsilon(\vec{r})$ is constant through space, eq. (1) leads to Coulomb's law

$$\varphi(\vec{r}) = \frac{1}{4\pi\varepsilon_0\varepsilon} \int_V \frac{\rho(\vec{r}')}{|\vec{r} - \vec{r}'|} d\vec{r}' \tag{2}$$

In the more general case where the dielectric function varies, for example due to a molecule boundary, a numerical solution to eq. (1) is necessary and can be obtained by various means, including the finite difference approach utilized in this work. Instead of eq. (2), the $\varphi(r)$ function can be recast in terms of a Green's function[13]

$$\varphi(\vec{r}) = \int_{V'} G(\vec{r}, \vec{r}')\rho(\vec{r}')d\vec{r}' \tag{3}$$

and the Green's function is the solution to this partial differential equation

$$\vec{\nabla} \cdot (\varepsilon_0 \varepsilon(\vec{r}) \vec{\nabla} G(\vec{r}, \vec{r}')) = -\delta(\vec{r} - \vec{r}') \tag{4}$$

where $\delta(\vec{r} - \vec{r}')$ is a Dirac delta function. From eq. (4), it is clear that the Green's function is uniquely determined by the dielectric function and the boundary conditions.

For molecular mechanics force fields, it is important to use an electrostatic term incorporating charge density that approxi-

mates well the ESP calculable from QM approaches. For this purpose, a set of point charges located at the nuclei positions is almost always used and the magnitude of the charges are often fitted to the QM ESP evaluated on a grid of points of outside the van der Waals (vdW) radius of the atomic nuclei. Looking again at the conventional constant dielectric case [eq. (2)], from Coulomb's law the charge density of a point charge is given by $\rho(\vec{r}) = \delta(\vec{r} - \vec{r}')Q$ and eq. (2) becomes:

$$\varphi(\vec{r}) = \sum_i^N \frac{Q_i}{4\pi\varepsilon_0\varepsilon|\vec{r} - \vec{r}_i|} \tag{5}$$

where the summation goes over the N point charges in the system. The standard procedures carry out the fit of the point charges using straightforward linear algebra techniques.[4–9] When there is a dielectric boundary, the problem must be recast to account for a variation of the dielectric function; we do this by rewriting eq. (3) for point charges.

$$\varphi(\vec{r}) = \sum_i^N G(\vec{r}, \vec{r}_i)Q_i \tag{6}$$

The task is now to optimize the Q_i charges to match the QM ESP, but the Green's function specific to the studied system remains to be determined. The key is to realize that in the case where point charges are being used, the calculation of the ESP function only requires knowing the response at discrete $\vec{r}_i$ point charge positions [from eq. (6)] and then eq. (4) becomes:

$$\vec{\nabla} \cdot (\varepsilon(\vec{r})\vec{\nabla}G(\vec{r}, \vec{r}_i)) = -\delta(\vec{r} - \vec{r}_i) \tag{7}$$

The advantage here is that the algorithms normally used to solve Poisson's equation can be used to calculate the Green's function for each independent charge position given by the ESP for a system in which all the charges are set to zero except the one located at $\vec{r}_i$, which is set to one. Equation (7) then becomes Poisson's equation for this specific system, for which the dielectric function contains all the details of the full molecular system. We now define a charge-source potential

$$\Phi^i(\vec{r}) \equiv G(\vec{r}, \vec{r}_i). \tag{8}$$

In practice, we obtain $\Phi^i(\vec{r})$ on a grid of points as a solution to a finite difference approach and the charge-source potential can be calculated for an arbitrary position by interpolation. We now come back to the problem of finding the optimal set of charges posed by eq. (6) and define the ESP calculated at grid point position $\vec{r}_m$ as

$$\varphi_m = \sum_i^N \Phi_m^i Q_i \tag{9}$$

where $\varphi_m = \varphi(\vec{r}_m)$ and $\Phi_m^i = G(\vec{r}_m, \vec{r}_i)$. We have replaced the Coulomb's law of eq. (5) by a calculable response function

uniquely defined by the same dielectric function and the boundary conditions of the full Poisson's equation [eq. (1)]. The linearity of eq. (9) in the charges is clearly amenable to a linear system of equations as done with the ESP-fit procedure. From this point, the method unfolds in a manner similar to conventional approaches to ESP-fitting: the goal is to obtain a set of atomic charges that produces an ESP φ that best approximates that computed from an accurate QM calculation ψ. This is achieved by minimizing the sum of the squares of the residuals between φ and ψ, evaluated at each grid point m. Defining the residual as χ^2 we have:

$$\chi^2 = \sum_{m=1}^M (\varphi_m - \psi_m)^2 \tag{10}$$

Substituting eq. (9) into eq. (10) gives

$$\chi^2 = \sum_{m=1}^M \left(\sum_{i=1}^N Q_i\Phi_m^i - \psi_m \right)^2 \tag{11}$$

The values of Q_i that minimize the residual χ^2 are obtained by setting to zero the N first derivatives of eq. (11) against the atomic charges. This leads to:

$$\frac{\partial\chi^2}{\partial Q_k} = \sum_{m=1}^m 2 \left(\sum_{i=1}^N Q_i\Phi_m^i - \psi_m \right) \Phi_m^k = 0 \tag{12}$$

$$\sum_{i=1}^N Q_i \sum_{m=1}^M \Phi_m^i\Phi_m^k = \sum_{m=1}^M \psi_m\Phi_m^k \tag{13}$$

To simplify the notation, we define a matrix A and a vector b:

$$A_{ik} = \sum_{m=1}^M \Phi_m^i\Phi_m^k \tag{14}$$

$$b_i = \sum_{m=1}^M \psi_m\Phi_m^i \tag{15}$$

The linear system of equations to solve becomes

$$\sum_{k=1}^N A_{ik}Q_k = b_i \tag{16}$$

If the internal dielectric is set to 1 (i.e., no dielectric boundary between the molecule and vacuum) in the computation of charge-source potentials, then the linear equations in eq. (16) become

identical to those used by RESP[6] or other conventional methods.[4,5,7–9] However by introducing a dielectric boundary to model solute polarizability in the calculation of the charge-source potentials, it is possible to account for the contribution of polarization effects in obtaining charges that fit to the QM ESP. In general, one can solve Poisson's equation and interpolate the ESP on the fitting grid for each Green's function related systems. In practice, this procedure requires a solution per point charge. The introduction of the dielectric effects into the overall procedure is indicated by calling the modified procedure Dielectric RESP (DRESP).

It is also possible to incorporate Lagrangian constraints and regularizing restraints as with RESP[6]; the latter reduce the charge magnitudes to make them more transferable at the expense of reducing the fit quality. In this work, we chose not to use restraints whether using a dielectric of one (RESP) or higher (DRESP) so as to retain the best fit quality for comparison to the QM ESP. Charge transferability is taken care of with the AM1-BCC charging scheme. We did however constrain topologically equivalent atoms to have identical charges and applied a constraint to the molecular formal charge. For example, the high symmetry of benzene leads to only one charge degree of freedom whereas in 4-pyridone there are 7 such degrees of freedom. Finally, the general formulation presented here allows the use of any kind of dielectric boundary functions (smoothed or not) and multiple dielectric values.

Computational Details

Ab initio QM electronic calculations were all based on density functional theory (DFT) using the B3LYP[14–16] functional as implemented in the Gaussian 03[17] software. The molecular geometries were optimized as reported in a previous study[1] with a 6-31++G(d,p) basis.[18] Subsequent ESP and energy calculations were performed using these optimal geometries but with an extended 6-311++G(3df,3pd) basis set. Molecular symmetry was not used as part of the calculations and an accurate convergence criteria was specified for the iterative calculation of the electron density matrix (by using the keyword Scf = Tight, which sets the average density change to be smaller than 10^{-8} a.u.). Interaction energies reported in this work were all corrected for basis set superposition error (BSSE) using the Boys and Bernardi counterpoise method.[19,20]

Finite difference Poisson calculations were done using the program Zap.[21] A grid spacing of 0.5 Å was used to calculate potentials for both the DRESP charge fitting procedure and in the analysis of induced polarization. A smaller grid spacing of 0.3 Å was needed when solving PE to obtain smooth intermolecular energy curves. The grid boundary was positioned 10 Å away from the closest point on the vdW surface. The convergence grid energy was set to 0.00006 kcal/mol and a Richards vdW surface[22] was used to define the molecular dielectric boundary. The molecule inner dielectric and atomic radii were based on the parameterization that reproduced vacuum QM polarizabilities.[1] The three parameter sets reported previously[1] are examined in this work, namely: the "P2E" parameter set which adopts different dielectric values for alkane and aromatic molecules, the "P1E" parameter set in which a single dielectric is used to describe the solute response of all molecules, and

finally "Bondi" which combines a dielectric of four with Bondi radii[23] (H radius set to 1.1 Å). The P2E and P1E parameter sets use optimal radii which are systematically smaller than Bondi radii, necessary to accurately reproduce the anisotropy of the molecular polarizability.

The adaptation of charges from a vacuum-dielectric source to the EPIC polarization model used a vacuum-adapted AM1-BCC model as an example. A vacuum AM1-BCC model was developed based on conventional ESP-fitting of bond charge corrections as described previously,[10,11] except that QM ESP from B3LYP/cc-pVTZ wavefunctions were used instead of the conventional HF-6-31G* calculations. Using this AM1-BCC/vacuum model, charges are generated for a molecule as described previously[10,11]; these charges assume a uniform dielectric of 1 both inside and outside the molecule. With these atomic point charges, a new ESP is generated around the molecule using a face-centered cubic (FCC) grid ranging from 1.4 to 2.0 times the atomic Bondi vdW radii.[10,11] These distances have previously been determined to lead to an adequate sampling[24] of the ESP for atomic charge determination. The FCC grid spacing was set to 0.5 Å. This ESP, called the AM1-BCC/vacuum ESP, is now input to the DRESP method to generate charges for the same molecule only now incorporating the high inner dielectric and the dielectric boundary for the EPIC polarizable model. Both the AM1-BCC/vacuum ESP and the derived DRESP ESP may then be compared to the QM ESP for that molecule to give an RRMSD.

Induced Polarization

To examine the accuracy of the dielectric polarization model, molecules were probed with a +0.5e point charge positioned exterior to the vdW surface of molecules. This probe charge has been used by others[25,26] and was recently shown to be well-adapted to examine the polarizability of aromatics.[26] In this work, the probe charge positions were determined using a single Conolly surface[27] with a vdW distance scaling factor of 2.0 and a density of 0.4 point per Å². Redundant probe charge positions, by symmetry, were partially eliminated. For example, this resulted in benzene having six positions for the perturbing charge, whereas 1,2,4-triazine had 47.

The induced potential is obtained by difference relative to the vacuum potential. Care must be taken to eliminate the contribution of the perturbing point charge to the calculation of the induction potential. This is handled automatically in the QM case as a consequence of the coding of Gaussian03. However, when using Zap an extra calculation is required to determine the explicit Coulombic potential arising from the perturbing charge. In total, the induced potential required three PE solutions per molecule on a constant grid. The numerical accuracy was ensured with the low energy convergence criterion.

The difference between QM induction potential (ψ) and that from EPIC model (φ) is characterized as a relative root mean square deviation (RRMSD) as follows:

$$\text{RRMSD} = \frac{\sum_{m=1}^{M}(\psi_m - \varphi_m)^2}{\sum_{m=1}^{M}(\psi_m)^2} \qquad (17)$$
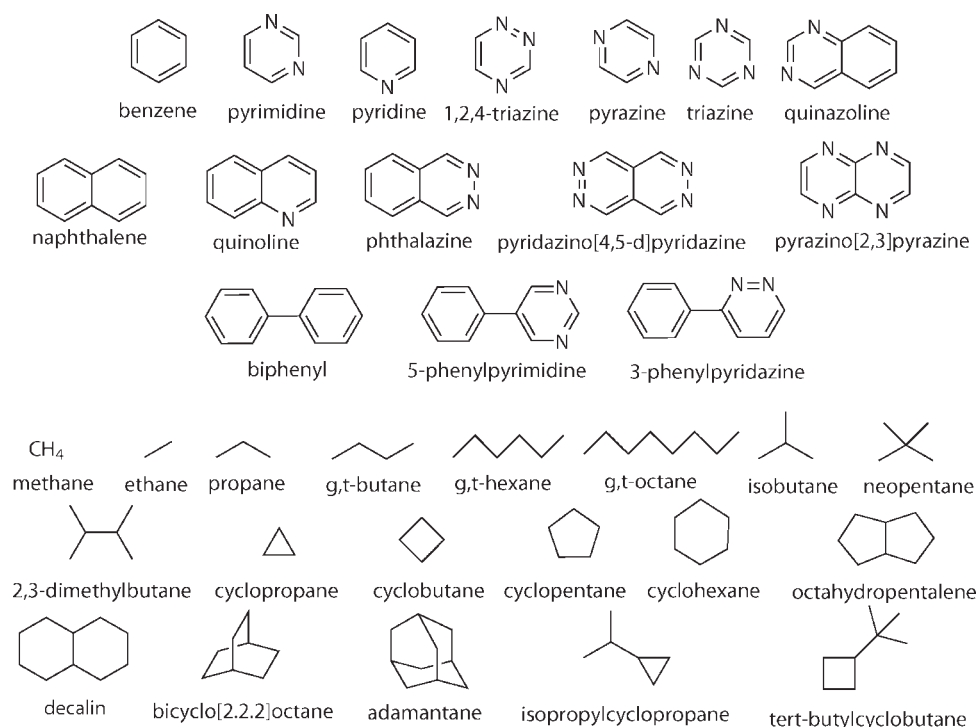
Figure 1. Molecule dataset which contains aryls and alkanes chemical classes. These 15 aromatic and 21 alkane molecules are extracted from reference 1. We use the notation "*t*" to indicate the all-trans conformation and "*g*" when one or more gauche dihedrals are present; these are separate entries.

Molecule Dataset

The molecule dataset used in this work contains 15 polar and nonpolar aromatics and 22 alkanes as shown in Figure 1. In addition, 4-pyridone is used in the study of a H-bond potential. The aromatic molecules exhibit quite a large spectrum of values for the ESP at the surface studied and possess a wide range of polarity. Due to their anisotropy, they constitute a good challenge to polarizable methods. Because of their nonplanarity, biphenyl and its analogs have a different shape of the potential and a different conjugation of the π electron system compared to the other aryl molecules. Finally, the alkanes are quite polarizable despite their low polarity and the molecules used explore many kinds of shapes. All the molecule structures in this dataset are from the previous study.[1]

Results and Discussion

In this section, the ability of the proposed least-squares fitting method, DRESP, to produce an accurate permanent ESP is first examined and compared to the least-squares ESP-fitting. We then continue by proposing a general way of coupling an existing charge model to EPIC, illustrated with the AM1-BCC charge model, which is general and shows many advantages in condensed phase simulations.[10,11,28,29] The ability of the EPIC approach to produce an accurate induced ESP in the presence of a locally varying electric field is also examined. Finally, the polarizable and permanent features of EPIC are used to study the electrostatic energy profiles in two challenging cases: cation-π and 4-pyridone H-bonded dimers.

DRESP vs ESP-Fit

Given the way EPIC incorporates electronic polarization through a dielectric boundary coupled with a high inner dielectric, the usual strategy to fit atomic partial charges to reproduce the QM *ab initio* ESP was modified to make DRESP as described in the methods section. We first apply DRESP with the P2E parameters and compare the RRMSD made on the permanent ESP of B3LYP for the molecules of Figure 1. The atomic partial charges are also fitted to the same vacuum QM ESP using the conventional internal dielectric of 1, denoted "ESP-fit", which has no dielectric boundary. A consequence of the dielectric screening with high inner dielectric is that DRESP charges are significantly larger than those obtained with the ESP-fit. This is illustrated in Figure 2 for benzene, pyridine and cyclopropane: the C/H charges of benzene are found to be ± 0.12e as calculated by ESP-fit and ± 0.61 with the dielectric P2E model calculated with DRESP; the charges on pyrimidine are also significantly smaller with ESP-fit than with DRESP and similarly for cyclopropane. While the DRESP charges seem large and chemically counter-intuitive, they produce a comparable ESP to the conventional ESP-fit approach. Figure 2 also reports comparable RRMSD deviations between DRESP and ESP-fit for benzene, pyridine and cyclopropane. The RRMSD reported on cyclopro-
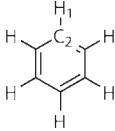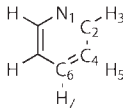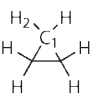
	Q_{ESP}	Q_{DRESP}
H_1	0.12	0.61
C_2	-0.12	-0.61
RRMS	14%	11%

	Q_{ESP}	Q_{DRESP}
N_1	-0.72	-2.56
C_2	0.57	1.49
H_3	0.01	0.24
C_4	-0.64	-1.26
H_5	0.21	0.60
C_6	0.39	-0.20
H_7	0.05	0.62
RRMS	13%	13%

	Q_{ESP}	Q_{DRESP}
C_1	-0.28	-0.72
H_2	0.14	0.36
RRMS	66%	54%

Figure 2. Benzene, pyridine and cyclopropane optimal charges fitting equally the same electrostatic potential with a dielectric of one (ESP-fit, nonpolarizable) and the P2E model (DRESP). The significantly higher charges with the P2E model comes from the internal dielectric screening of the point charges.

pane is high, but it is known that for simple alkanes the atomic partial charge approximation is poor.[30,31] However, since the actual ESP for the alkanes is very small, this defect might be negligible in intermolecular interactions although the alkane polarizability is not. Finally, it is important to keep in mind that whenever a radius or an inner dielectric value changes, the DRESP charges cannot be transferred but must be reoptimized against the same QM *ab initio* ESP grid.

Adapting an Existing Charge Model: The AM1-BCC/ DRESP Example

Here we give proof-of-concept for a method to translate atomic charges generated using a conventional ESP-fit approach into charges suitable for EPIC polarization. The approach taken here uses the AM1-BCC/vacuum charges to which dielectric-adapted charges are then fitted using the DRESP method as described in the Methods section. We call this fitting strategy AM1-BCC/ DRESP. Although we apply this strategy to the AM1-BCC/ vacuum charging scheme, it is general in the sense that any other uniform-dielectric-derived charge model could be adapted the same way. A key point is that the conventional ESP-fit charges used as a starting point must not be already over-polarized compared to vacuum; since most current charge models used for nonpolarizable biomolecular force fields are already over-polarized, special care must be taken in using the approach described above. It is for this reason that in the work described here we use a vacuum-adapted AM1-BCC, developed based on B3LYP/cc-pVTZ QM calculations (c.f. "Methods" section), instead of the over-polarized HF-6-31G* wavefunction usually used for charge-fitting for non- PFFs.

In Figure 3, we compare RRMSD for the fit to the B3LYP/6-311++G(3df,3pd) ESP for both the AM1-BCC/vacuum and the AM1-BCC/DRESP ESP. The correlation is excellent for aromatics and the AM1-BCC/DRESP charges produce slightly smaller RRMSD for the alkanes, which we think is not significant given the low level of accuracy for this chemical class. This demonstrates that extending an existing charge model,

developed in a nonpolarizable context, is easy and accurate. More importantly, the parameterization of the polarizable parameters and of the permanent charges can be fully decoupled, hence greatly reducing the fitting complexity.

Induced ESP

Previously, EPIC was shown to reproduce accurate induced dipole moments on molecules submitted to a uniform electric field.[1] Here we assess the ability of the approach to account for more local perturbations. This is accomplished by examining each of the 37 molecules from Figure 1 for which the ESP induced by a single probe charge of +0.5e is calculated with both B3LYP and EPIC according to the prescription detailed in the Methods section. Given the numerous placements of the probe charge for each molecule, the RRMSD deviations between B3LYP and EPIC are averaged and reported in Figure 4. This includes around 1700 B3LYP single point calculations in total. The RRMSD standard deviation (STDEV) indicates how much the error varies as a function of the position of the probe charge. The three bars per molecule correspond to the results obtained using three different parameter sets from the previous study.[1] The average RRMSD obtained with P2E (c.f. "Method" section) were used to sort the molecules in Figure 4. This method led to an average RRMSD and STDEV across the molecules of 1.06% and 0.3% respectively; the maximum average RRMSD is attributed to methane with 2.1%. The results obtained with the P1E parameter set (see "Method") are slightly worse with an average RRMSD across the molecules of 1.70% and a STDEV of 0.8%. In the case of the Bondi parameter set (see Method), the average RRMSD and STDEV are 3.74% and 2.0%, almost a factor of four higher than P2E. The errors reported with Bondi parameters
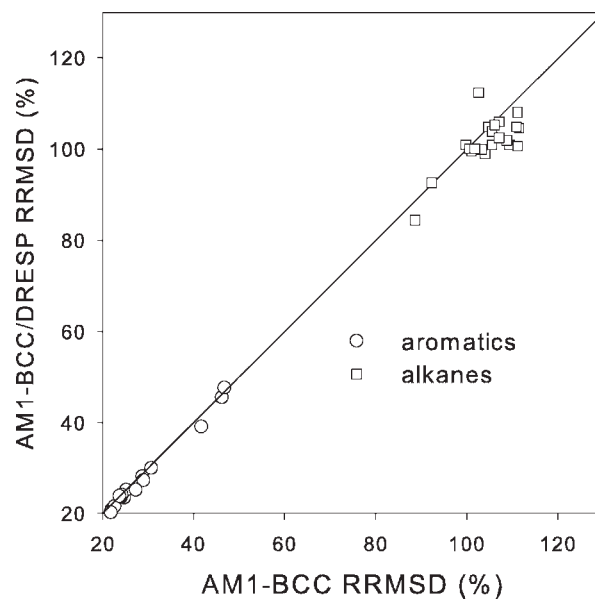

Figure 3. Correlation plot of the RRMSD obtained with AM1-BCC and AM1-BCC/DRESP charging schemes. The RRMSD are calculated against the B3LYP permanent electrostatic potential on the FCC grid.
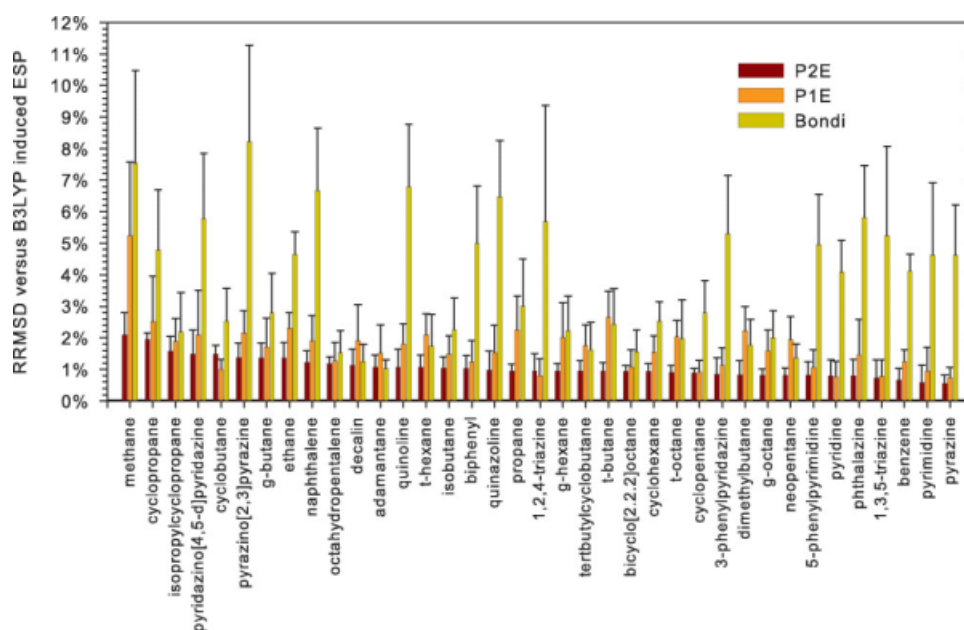
Figure 4. Average RRMSD on the induced ESP maps as calculated with EPIC using three parameter sets (P2E, P1E, and Bondi, see text). The ESP maps are generated by a +0.5e charge located at non-redundant positions and the reference induced ESP is calculated from B3LYP 6-311++G(3df,3dp).

show a bias toward a more accurate description of the alkane polarizabilities.

To examine the effect of induction by the +0.5e charge on the alkanes, nonpolar aromatics, and polar aromatics, it is of interest to compare the grid unsigned average of the induced and vacuum ESPs for each class. In the case of the alkanes, the unsigned average of the induced ESP is about 3 times higher than the vacuum ESP evaluated on the fitting grid. Benzene and nonpolar aromatics have comparable induced and static ESP positive magnitudes and, in the case of polar aromatics such as pyrimidine, the induced ESP is between twofold and threefold smaller than the vacuum ESP. This indicates that the level of electronic polarization is significant and appropriately challenging to the polarizable model. The RRMSD obtained with the induced ESP is much lower than the RRMSD of the static ESP fit by atomic charges. This shows that the model can accurately account for locally induced polarization although the induced ESP is certainly simpler than the ESP originating from the unperturbed molecule.

Here, we use the induced ESP to test the ability of the EPIC model, parameterized solely on the QM gas phase polarizability tensor, in reproducing a molecule's induced QM electronic response to a polarizing charge. The very small RRMSD obtained with the P2E and the P1E parameter sets indicate that the local polarization with a nonuniform electric field is as accurately modeled as the induced dipole moment due to a uniform electric field[1] (molecular polarizability), the basis of the P2E and P1E parameterization. In contrast, most previous polarizable models[32–34] obtain their polarizability parameters (and often simultaneously the charges) by fitting to the induced ESP on polarized molecules.
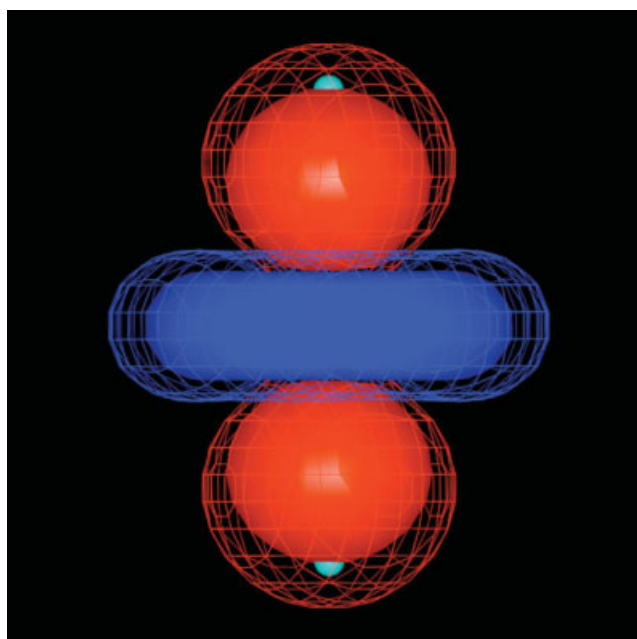

Figure 5. The induced electrostatic potential of an argon atom sandwiched in between two +0.5e charges positioned at 3.0 Å from the nucleus. The solid iso-surface corresponds to the B3LYP/6-311++G(3df,3pd) and the mesh iso-surface to the result from EPIC (radius = 1.3 Å, dielectric = 7.4). The induced moment is an induced quadrupole with the d_z^2 orbital symmetry. The traditional atomic polarizable approaches have a zero induced electrostatic potential.

Induction by a Symmetric Field

The parameterization of polarizable models usually involve simple fields such as uniform external electric fields or fields produced by a probe point charge or a probe dipole. These external fields induce mainly a molecular dipole moment, which should be reasonably well accommodated given a simple functional form for a polarizable model. However, in condensed media, the electric field is rarely simple and is often transiently symmetric around a molecule. In this section we compare the induced ESP in a nontrivial electric field applied on an argon atom and benzene; three methods are examined: point inducible dipoles, EPIC and B3LYP.

In the first system, the argon atom is sandwiched between two point charges positioned at 3.0 Å above and below the atom. The EPIC argon radius used is set to 1.31 Å and the dielectric = 7.36 as fit to reproduce the (gas-phase) B3LYP atomic polarizability of argon (11.1 a.u.). Given the symmetry of this system, the net electric field at the argon nucleus is zero. Since the point inducible dipole[1] and the fluctuating charges[35] polarizable models respond only to the net electric field at the nucleus, neither of these models would show induction in this case. As illustrated on Figure 5, the B3LYP induced ESP is a quadrupole with the d_z^2 hydrogenoid-like orbital symmetry. Remarkably, the EPIC induced ESP has the same symmetry and is of similar magnitude.

The second system examined consists of benzene sandwiched by two +1e point charges located at 2 Å above and below the ring along the symmetry axis. This is a fairly large perturbation where the point charges are positioned approximately at the Li^+/benzene equilibrium distance. Although in nature it is unlikely that two Li^+ atoms would be stable in such a sandwich system, the perturbing electric field varies quickly from zero at the center of the benzene ring to 2/r at infinity. So within the volume of the benzene, the field varies enough to significantly test the model. The symmetry of this arrangement is such that the external electric field has only a component in the plane of the ring at the atomic positions, although the out-of-plane polarization should be predominant. A similar system was used to show the failure of the fluctuating point charges model by Stern et al.[35] In principle the point inducible and related polarizability models should also have difficulty since the magnitude of the induced potential would then be fully dictated by the in-plane polarizability component. For our comparison, we used the AMOEBA polarizability model for benzene which includes a Thole exponential damping parameter of 0.39 coupled with carbon and hydrogen isotropic polarizabilities of 1.334 Å^3 and 0.8 Å^3 respectively (as provided in TINKER 4.2 distribution parameter file). The Thole parameter has the role of adjusting the molecular polarizability anisotropy by reducing the atomic induced-dipole/induced-dipole interactions thereby avoiding the polarizability catastrophe, inherent to the PID models. Calculated with these parameters, the benzene vacuum molecular polarizabilities are 11.4 Å^3 in the plane and 6.2 Å^3 perpendicular to the plane, which are in close agreement with the values of 12.2 Å^3 and 6.7 Å^3 obtained with B3LYP/aug-cc-pVTZ. For this comparison, we use EPIC with the P2E parameters which also produces accurate polarizabilities of 12.2 Å^3 and 6.6 Å^3.

For the charge-sandwiched system, the iso-contour lines of the induced ESP on one of the six planes of symmetry perpendicular to the ring are plotted in Figure 6. The iso-lines are spaced by 5 kcal/mol/e and the ESP values are given in kcal/mol/e. For the three methods, the induced ESP has the shape and symmetry of a d_z^2 orbital, a quadrupole moment, with the negative lobes oriented along the axis joining the two probe charges and the positive torus located close to the hydrogen atoms. Good agreement is obtained between the induced ESP of B3LYP and EPIC even intramolecularly. At the probe charge positions, the B3LYP, EPIC, and AMOEBA induced potentials are −52, −60, and −29 kcal/mol respectively. In general the point inducible dipole potential is too positive moving away from the benzene along the probe charge axis. The relatively large difference between B3LYP and AMOEBA, compared with the smaller error made with EPIC, cannot solely be explained by the smaller in-plane benzene polarizability of AMOEBA because the AMOEBA positive ESP regions, particularly at vdW distances from the H atoms (2 Å away), match the B3LYP values. We attribute the better success of the dielectric-based EPIC model to its departure from the atomic nucleus-centric polarization to an atomic volume-centric model where the entire molecular boundary responds to the electric field. To improve the PID model while retaining the correct average molecular polarizability and anisotropy of benzene, auxiliary polarizable points above and below the ring would have to be added, at the expense of additional complexity and supplemental parameterization. This being said, condensed phase simulations have lead to parameterizations of polarizable PID-based force fields that accounted for important liquid properties of benzene[36] although a polarizable electrostatic term is often not necessary to fit the liquid properties. We believe that the accurate polarizable electrostatic term should make a more important difference in an heterogeneous and anisotropic environment such as the active site of an enzyme or a trans-membrane ionic channel. It is encouraging that the EPIC model with default P2E parameters from the gas phase exhibits good physical behaviors at the purely electrostatic level even in the context of strong and complex electric fields.

Cation-π Interactions

In the previous sections, we have separately demonstrated that EPIC can handle both the permanent and induced ESP strictly by comparison to the induced B3LYP ESP s. Now, we combine charges from the DRESP fitting procedure and polarization from the EPIC model to assess the electrostatic interaction energy in cation-π systems. The cation-π attractive interaction energy between benzene and Li+, Na+ or K+, displaced along the benzene six-fold symmetry axis, was shown to be impossible to describe with nonpolarizable models.[37] However, the contribution of the induction energy (from electrostatic polarization) is crucial for an accurate description of cation-π binding.[37,38] Furthermore, the presence of cation-π interactions in many biological systems[39–41] makes this application a critical validation for a new polarizable electrostatic term. Therefore, in this section we decompose the total interaction energies and check if the induction found with the P2E parameter set is quantitatively correct.
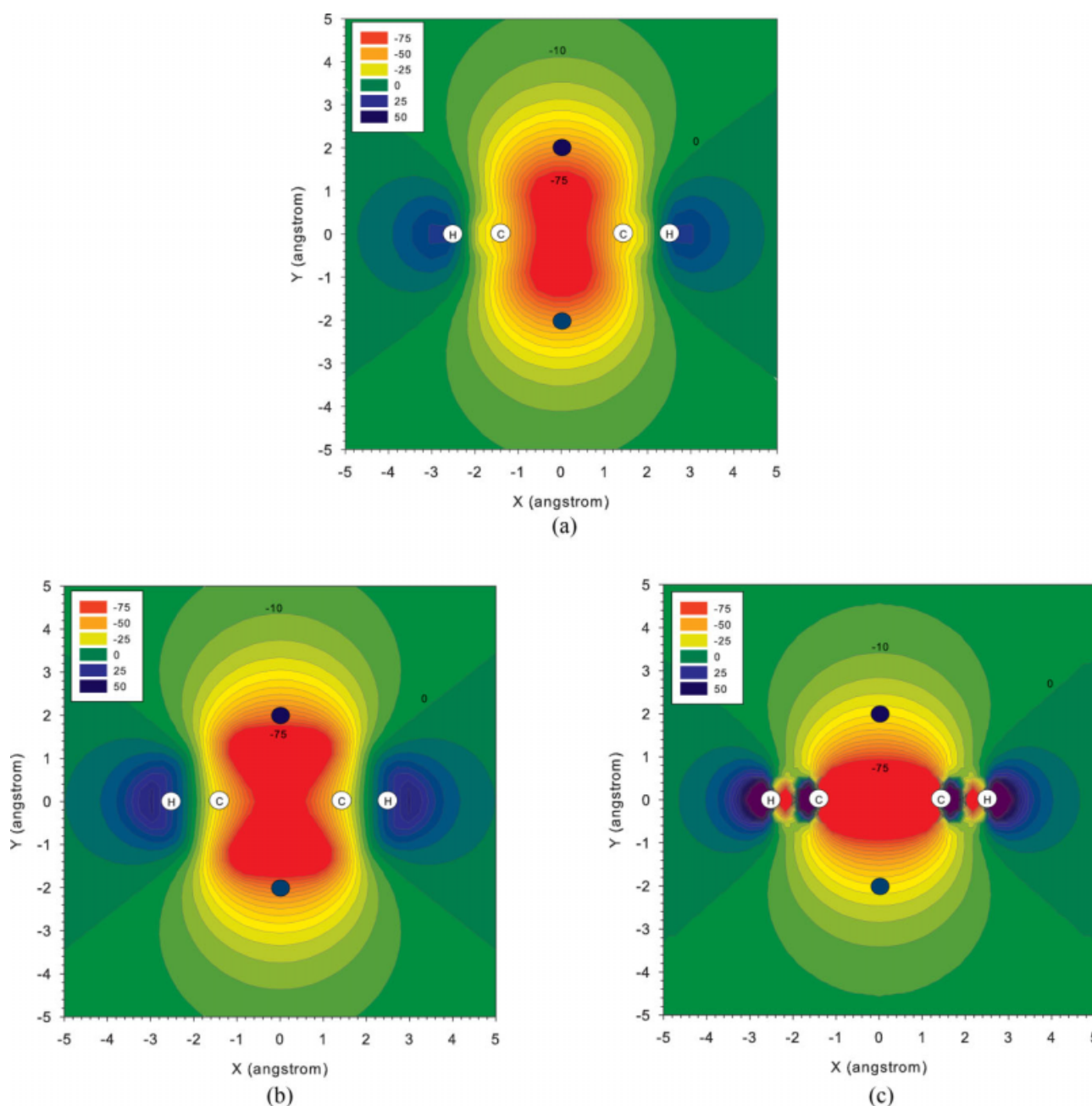
Figure 6. The induced electrostatic potential for benzene is shown by iso-contour lines spaced by 5 kcal/mol on one of the six symmetry plan perpendicular to the ring. The external perturbing potential is produced by two $+1e$ charges positioned 2 Å above and below the benzene ring. The induced potential obtained at the B3LYP/6-311++G(3df,3pd) level (a) is compared to the EPIC/P2E (b) and AMOEBA, a good quality QM derived point-inducible model (c).

At the QM level, the total interaction energy between an atomic cation and benzene can be conceptually split into electrostatic, vdW repulsive, and vdW attractive components. Each term is normally represented separately in a force field, although one term often compensates for another containing deficiencies. We are now only interested in examining the electrostatic component and we focus on the proton since its vdW interaction with the benzene can be neglected. Other cations have similar electrostatic profiles outside their vdW range (data not shown). At the force field level, if the proton/benzene interaction energy is described correctly, all that remains to be added is the repulsive vdW term to model other, more physiologically relevant,
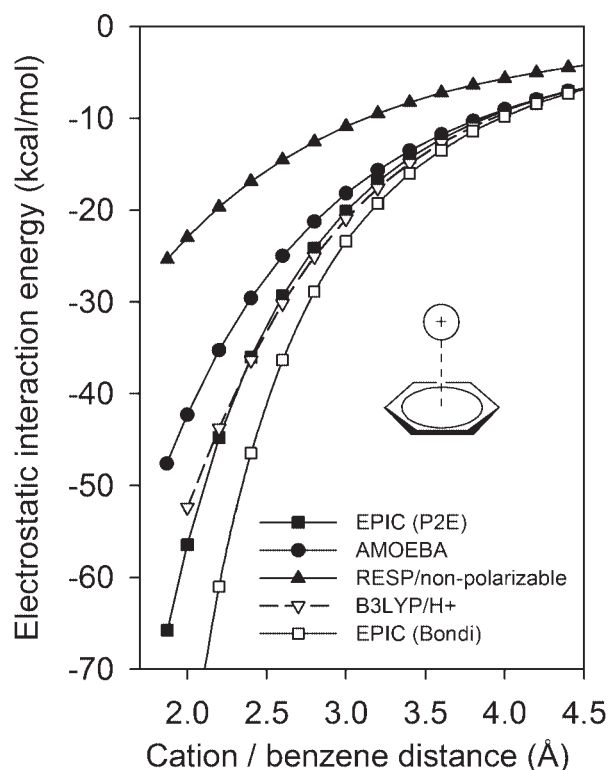
Figure 7. The electrostatic interaction energy between a benzene molecule and H+ displaced along the C_6 symmetry axis corresponds to the electrostatic component of a cation-π system formed with an atomic cation. The nonpolarizable model using ESP derived charges is far from the B3LYP calculated energy, the EPIC/P2E model closely follows the B3LYP curve and AMOEBA captures most of the electronic polarization of B3LYP. The EPIC electrostatics fitted on B3LYP monomer reproduces the correct cation-π electrostatic energy without adjustment.

atomic cation-π interactions. This will be shown in the next section in a different application.

The energy of interaction between a benzene molecule and H$^+$ placed above the ring along the symmetry axis is calculated at the B3LYP/6-311++G(3df,3pd) level with no basis function positioned on the proton to avoid unphysical stabilization. Figure 7 reports the energies as a function of the distance from the center of the benzene ring using B3LYP, a nonpolarizable Coulomb potential calculated with RESP-fitted atomic charges, the electrostatic component of the polarizable AMOEBA force field, and the polarizable EPIC/P2E model. For the nonpolarizable and AMOEBA models, the parameters mentioned in section 3.4 are used. Figure 7 shows that EPIC matches quantitatively the B3LYP energy profile. As found previously,[37] the nonpolarizable potential is inappropriate for describing cation-π interactions, despite the fact that the atomic partial charges of benzene were fitted on the same ESP grid as were the EPIC/DRESP charges. The energy resulting from electronic polarization dominates the electrostatic interaction energy, being twice more stabilizing than the static contribution at typical intermolecular separations. This induction energy remains substantial for intermolecular separa-

tions as large as 4 Å. The AMOEBA description of the electrostatic energy captures most of the induction energy. This model, like EPIC, is derived from *ab initio* calculations, but includes atom-based multipole expansion terms up to the quadrupole for the permanent potential. In addition, AMOEBA adds an atomic polarizability on the hydrogen atoms. The difference between B3LYP and AMOEBA energies can be explained, in part, by AMOEBA's slightly smaller out-of- plane polarizability (c.f. section 3.4). Tsuzuki et al.[38] have shown that it is possible to get the cation-π system correctly modeled with a PID model if it is parameterized in a specialized manner. In their work they not only use atomic multipoles, but also anisotropic atomic polarizability located on the carbon atoms. Once more, we see that the EPIC model with P2E parameters is robust and general, needing only a small number of default parameters to account for the different aspects of electronic polarization. The accuracy of this model implies that the vdW term will not need to compensate for errors in the close-range electrostatics thus easing its parameterization.

H-bond of the Pyridine-4(1H)-One Dimer

The induction energy in H-bonds is implicitly included in existing additive force fields. The single-minimum interaction energy profile representing an H-bond becomes a trade-off between the attractive electrostatic term and the short-range repulsive vdW term of a force field. For example, in the original AMBER force field a special 12–10 Lennard-Jones potential was initially needed to describe short range H-bonding potentials.[42] In more recently developed non-PFFs,[43] both the condensed phase overpolarized HF/6-31G(d) charges and the addition of hydrogen atom types using small Lennard-Jones radius (σ) parameters corrected for the lack of induction energy. Including explicitly induction energies should, in principle, simplify the parameterization of vdW potential and incorporate nonadditive condensed phase effects such as H-bond cooperativity.[44,45] In this section, we examine the challenging case of pyridin-4(1H)-one, hereafter 4-pyridone, which was shown to form strong intermolecular H-bonds[46] when monomers are coplanar and aligned along the two-fold axis passing through the NH and the CO bonds. This is in part due to the large dipole moment of 7 Debye and the high polarizability component of 97 a.u. both oriented along the H-bond axis that should polarize the monomers and thereby constitute an interesting second application for the validation of polarization using EPIC. This is a case where polarizability needs to be taken into account even at the dimer level. In what follows, we conduct two different studies which objectives are (a) to assess if the EPIC model with DRESP charges gives the correct electrostatic interaction energy profile compared to B3LYP and (b) to reproduce the dimer H-bond dissociation energy curve obtained by B3LYP.

1 4-*pyridone Dimer Electrostatic Interaction Energy*

Unlike the previous cation-π application, evaluating the performance of our electrostatic approach here involves partitioning the total electronic structure energy into its components because the vdW term cannot be neglected. We will divide the total energy into an electrostatic (ΔEelec) term and an exchange-repulsion (hereafter called the vdW repulsion and noted ΔEvdw) term.
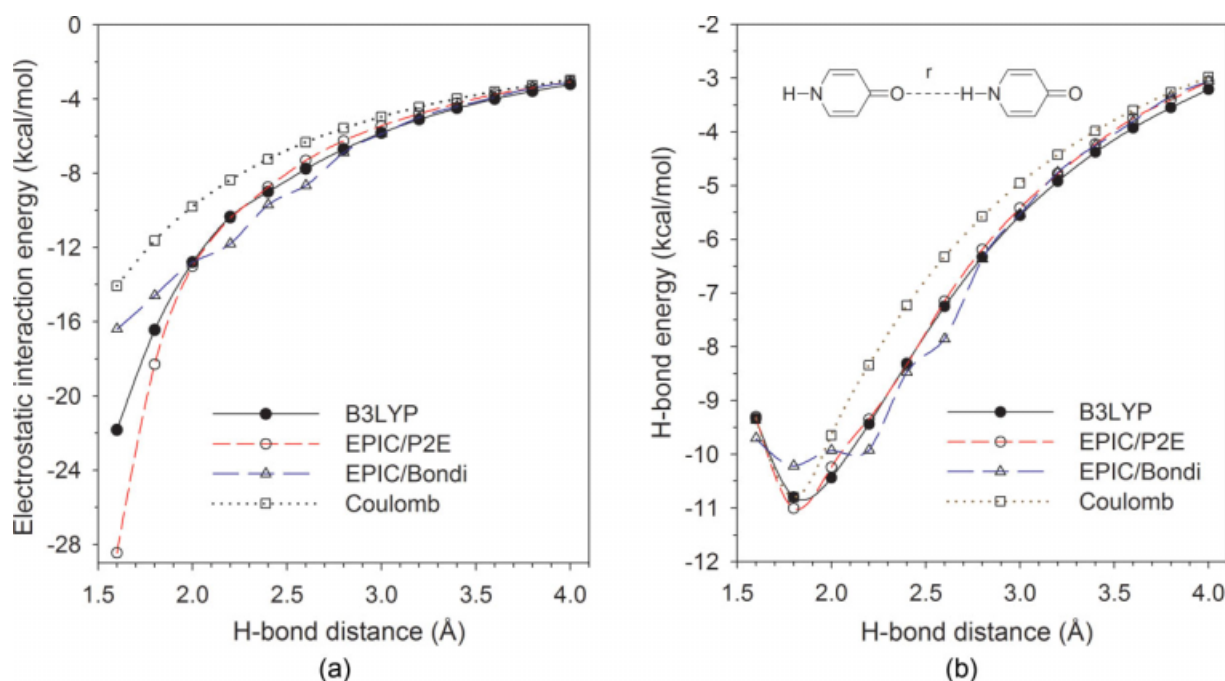
Figure 8. The reported electrostatic interaction energies of the H-bonded 4-pyridone dimer (a) show that the EPIC/P2E model produces the appropriate polarization as opposed to the nonpolarizable permanent charge model (Coulomb) when compared to B3LYP [eq. (19)]. The EPIC/Bondi calculations produce the correct electronic response at long ranges of H-bond distances but saturates as the vdW dielectric surfaces of the monomers start overlapping. The observed deviations are a result of the numerical instability that occur when the dielectric spheres come into contact at 2.6 Å. (b) The BSSE/corrected B3LYP interaction energies of the dimer unveils a very strong H-bond of −10.8 kcal/mol at the minimum located at 1.78 Å. The reported classical approaches combined the electrostatic energies (shown in a) and a fitted repulsive vdW term. EPIC/P2E matches the B3LYP energies over the examined range whereas the Coulomb nonpolarizable model deviates at longer distances as a result of the difficulty for such a model to match both regions. [Color figure can be viewed in the online issue, which is available at www.interscience.wiley.com.]

The short range attractive dispersion energy is omitted because B3LYP does not capture it and it remains very small compared to the range of energies involved.

Given this partitioning, we calculate ΔEelec by subtracting ΔEvdw from the total interaction energy (ΔEtot). The delta symbol in front of the energy signifies that this is an interaction energy, meaning the difference in energy between the interacting system and the energies of the monomers. To approximate the $\Delta E\text{vdw}^{\text{DFT}}$ term, we used benzo-1,4-quinone (quinone) and benzene which both have a relatively small ESP. The benzene hydrogen replaces the 4-pyridone H donor and the quinone oxygen the acceptor, forming a quasi H-bond. The assumption here is that the vdW repulsive term is similar between the two systems. The monomer geometries are held fixed and the carbonyl oxygen to benzene H distances are the same as the 4-pyridone H-bonded dimer distances. The ESP of both molecules is relatively small and can be approximated using RESP-derived atomic point charges ($\Delta E\text{elec}^{\text{ESP}}$); thus ΔEelec is calculated using eqs. (18) and (19):

$$\Delta E\text{vdw}^{\text{DFT}} \approx \Delta E\text{tot}^{\text{DFT}}(\text{benzene, quinone})$$
$$- \Delta E\text{elec}^{\text{ESP}}(\text{benzene, quinone}) \quad (18)$$

$$\Delta E\text{elec}^{\text{DFT}} \approx \Delta E\text{tot}^{\text{DFT}}(\text{4-pyridone, 4-pyridone})$$
$$- \Delta E\text{vdw}^{\text{DFT}} \quad (19)$$

Figure 8a shows $\Delta E\text{elec}^{\text{DFT}}$ (B3LYP), $\Delta E\text{elec}^{\text{ESP}}$ (Coulomb), and $\Delta E\text{elec}^{\text{DRESP}}$ (EPIC) associated with the 4-pyridone dimer for distances going from 1.6 to 4 Å. The the equilibrium distance is found at 1.78 Å[46]; details of the energies are reported in the Supporting Information. As reported in Figure 8a, the induction energy stabilization obtained with EPIC/P2E matches B3LYP over most of the distances. The deviations at close contact (<2 Å) may be attributable to defects in the approximation given by eq. (18). Comparing the Coulomb and B3LYP curves at the equilibrium distance, the induction energy is almost −5 kcal/mol, a significant increase over the Coulomb value of

−11.6 kcal/mol. The quantitative match between the approximated B3LYP electrostatic H-bond energy shows that the induction interaction is appropriately described by our polarizable EPIC/P2E. It is important to emphasize that the radii and dielectric parameters (P2E) used were not fitted to any energy but to the QM gas-phase molecular polarizability tensors for many molecules simultaneously.[1] In Figure 8a, we can also see the EPIC/Bondi interaction curve that uses DRESP derived charges and the Bondi parameter set (c.f. Method). The long range interaction energies are appropriate but when the electronic volumes, defined by the Bondi radii (1.52 Å for oxygen and 1.1 Å for the hydrogen), start to interpenetrate, the induction energy becomes insufficient and undergoes numerical instability that we attribute to the vdW surface used in the finite difference PB solver, known to form cusps.

2 4-pyridone Dimer Dissociation Energy

To get an idea of how well EPIC polarization could be incorporated into an atomic force field, a vdW term was fitted to see how well the QM energy profile could be reproduced; the details of the fitted vdW terms are given in the Supporting Information. The resulting complete interaction energy profiles for the H-bond formation of the 4-pyridone dimer, $\Delta E\mathrm{tot}$(4-pyridone,4-pyridone), are presented in Figure 8b. For the DFT profile ($\Delta E\mathrm{tot}^{\mathrm{DFT}}$), the approximation of eq. (19) is not needed because only the total energy is examined. The B3LYP/6-311++G(3df,3pd) BSSE corrected energies show a very stable H-bond with a dissociation energy of −10.8 kcal/mol.

A few comments on the vdW fitting process are in order. In keeping with high-level QM calculation of exchange-repulsion energies,[43] we have used a two-parameter exponential vdW energy function $\Delta E\mathrm{vdw}^{\mathrm{EPIC}}(r)$ fitted to the residuals $\Delta E\mathrm{tot}^{\mathrm{DFT}}(r)$ − $\Delta E\mathrm{elec}^{\mathrm{EPIC}}(r)$ calculated along the intermolecular H-bond axis. Fortunately, the vdW dispersion energy, an attractive force, is absent in DFT methods and should not be needed here. The fit of the EPIC/P2E residuals resulted in a dissociation energy curve quantitatively reproducing the B3LYP energies in all ranges examined, giving a correlation coefficient (R^2) of 0.999. Note that the atomic partial charges derive from a DRESP fit to the monomer only. In contrast, the Coulomb model residuals (using atomic partial charges from the gas-phase monomer without polarizability) could not be fit to an exponential as successfully, exhibiting an attractive potential well of about −1 kcal/mol located at 2.3 Å (see Supporting Information). This example shows that, at the level of the dimer, the lack of polarizability introduces a requirement for a more complex functional form for the vdW term to compensate. Finally, the EPIC/Bondi potential has difficulty capturing the energy minimum and exhibits numerical instability. At very short H-bond distances (<1.5 Å), EPIC/P2E also exhibits similar instability behavior, but fortunately this is less relevant given that the high repulsive vdW energy is dominant. This is due to the smaller dielectric radii assigned to the oxygen and hydrogen atoms in the fit. The use of a smooth dielectric boundary could significantly reduce these effects.[21]

While these applications demonstrate the use of EPIC to incorporate electronic polarization into short-range intermolecular interactions, the generalization of this model for use in the condensed phase will require special attention in the parameterization. Indeed, it has been proposed based on various evidence that the condensed phase molecular polarizability per monomer is smaller than its gas phase polarizability. In practice, the correction to a PID model was made by fitting the polarizabilities on *ab initio* values obtained with a relatively small basis set, which systematically produces smaller molecular polarizabilities.[47] Hence for the PID model, the parameterized polarizability cannot accurately account for both the gas- and condensed-phase polarization, one of the main objectives for a PFF. We are currently examining this problem with EPIC and this will be addressed in a subsequent publication.

Conclusion

This work extends the proof-of-concept of the EPIC (electronic polarization from the internal continuum) approach to intermolecular interactions.[1] We show that in general the presence of an intramolecular continuum dielectric, for example in PB or PE formalisms, requires a modification of the conventional method for obtaining accurate atomic partial charges. We derive a least-squares approach called DRESP, by analogy to RESP, which not only reproduces the *ab initio* ESP but also offers a way to transfer the atomic partial charges from an existing vacuum charge model. We demonstrate this by successfully transferring the charges from an AM1-BCC/vacuum charging scheme of a set of 37 molecules including polar and nonpolar aromatics and alkanes. In general, the charges obtained are significantly larger whenever the dielectric inside the molecule is larger than one. Even more importantly, our results show that the polarizable parameters of EPIC can be derived independently from the permanent electrostatic terms. In fact, the atomic radii and dielectrics fitted to vacuum *ab initio* molecular polarizabilities were derived in the absence of atomic partial charges. We believe that this parameter decoupling will be an important asset to broaden the approach to encompass bio-organic chemistry.

Although EPIC was successfully fitted previously to reproduce *ab initio* dipole moments induced by a uniform electric field,[1] it was important to demonstrate that the full ESP induced by a more local or complex perturbation would be as accurate. To this end, we tested the validity of our parameters with a perturbing +0.5e probe charge moved on a Connolly surface. This is frequently employed to fit the polarizable parameters in force fields. The results were very encouraging leading to an average of 1% RRMSD deviation, relative to B3LYP, obtained from about 1700 calculations done on our set of 37 molecules. This shows that we can fit the EPIC radii and dielectrics on gas-phase molecular polarizabilities and expect an accurate local electronic polarization response as well.

A potential advantage of EPIC over other polarizable models is its use of "electronic polarizability density" through the intramolecular continuum dielectric. As opposed to PID models, the electric field induction is effective through the entire molecular volume. A recent study by Schropp and Tavan[48] suggests that the usual approximation that the polarizability is centered on atomic nuclei artificially invalidates the use of gas-phase derived atomic polarizabilities into condensed phase simulations unless nonobvious and nongeneral corrections are applied. To further

examine the ability of EPIC to deal with inhomogeneous environments, an argon atom and a benzene molecule were sandwiched by positive point charges. In both cases EPIC led to an accurate induced ESP relative to B3LYP. The *ab initio* derived AMOEBA PFF parameters were used for comparison and show a significant quantitative discrepancy of the out-of-plane potential. In agreement with Schropp and Tavan, we attribute this deficiency to the difficulty of atom centered polarizabilities to account for locally varying electric field.

We also applied our independently generated charges, radii and dielectrics to calculate the cation-π electrostatic interaction energy between a benzene molecule and a proton. This energy corresponds, more generally, to the electrostatic component for the binding of Li^+, Na^+ or K^+ to benzene where the induction energy is predominant. The results show that EPIC with parameters derived uniquely on the monomer led to B3LYP quality binding energies. In addition, the H-bonding electrostatic energy of the 4-pyridone dimer has been examined and we found that EPIC/P2E quantitatively matches the approximated B3LYP electrostatics and total interaction energies whereas the nonpolarizable term obtained with fixed charges derived from the ESP were not sufficient. Although we have not covered an exhaustive intermolecular list, these two applications are challenging cases that clearly show that the approach can work. Our fitting strategy of the electrostatic on the monomers can be easily generalized. In the 4-pyridone dimer example, we also show that the vdW term, needed to obtain the full energy, would not have to compensate for the poor electrostatics at short distances. This is one important and expected advantage from an accurate polarizable electrostatic model.

This work shows a new and potentially advantageous electrostatic term which could be applied to molecular dynamics or Monte Carlo simulations. Recently, molecular dynamics simulations using a PB solver to include implicitly the effects of solvent polarization were successfully carried out.[2,3,21,49–52] To fully use the concepts discussed herein as the electrostatic foundation of a force field, there remain scientific points to be addressed. The dielectric boundary will require special attention if stable forces are to be calculated. Also, transferability of the parameters obtained from *ab initio* gas-phase calculations to the condensed phase needs to be addressed. The extension of the parameterization will command a major effort not only for the electrostatic term, but also for all the other force field terms which need to balance the electrostatics.

Acknowledgments

References

1. Truchon, J.-F.; Nicholls, A.; Iftimie, R. I.; Roux, B.; Bayly, C. I. J Chem Theory Comput 2008, 4, 1480.
2. Maple, J. R.; Cao, Y. X.; Damm, W. G.; Halgren, T. A.; Kaminski, G. A.; Zhang, L. Y.; Friesner, R. A. J Chem Theory Comput 2005, 1, 694.
3. Schnieders, M. J.; Baker, N. A.; Ren, P.; Ponder, J. W. J Chem Phys 2007, 126, 124114.
4. Breneman, C. M.; Wiberg, K. B. J Comput Chem 1990, 11, 361.
5. Besler, B. H.; Merz, K. M.; Kollman, P. A. J Comput Chem 1990, 11, 431.
6. Bayly, C. I.; Cieplak, P.; Cornell, W. D.; Kollman, P. A. J Phys Chem 1993, 97, 10269.
7. Storer, J. W.; Giesen, D. J.; Cramer, C. J.; Truhlar, D. G. J Comput Aid Mol Des 1995, 9, 87.
8. Tan, J. S.; Boerrigter, S. X. M.; Scaringe, R. P.; Morris, K. R. J Comput Chem 2009, 30, 733.
9. Carey, C.; Chirlian, L. E.; Francl, M. M.; Gange, D. M. Glycoconjugate J 1997, 14, 501.
10. Jakalian, A.; Bush, B. L.; Jack, D. B.; Bayly, C. I. J Comput Chem 2000, 21, 132.
11. Jakalian, A.; Jack, D. B.; Bayly, C. I. J Comput Chem 2002, 23, 1623.
12. Tan, Y. H.; Luo, R. J Chem Phys 2007, 126, 094103.
13. Arfken, G. B.; Weber, H. J. Mathematical Methods for Physicists, 6th ed.; Elsevier, Academic Press: New York, 2005.
14. Becke, A. D. J Chem Phys 1993, 98, 5648.
15. Becke, A. D. J Chem Phys 1993, 98, 1372.
16. Stephens, P. J.; Devlin, F. J.; Chabalowski, C. F.; Frisch, M. J. J Phys Chem 1994, 98, 11623.
17. Gaussian 03, Revision, version C.02; Wallingford CT, USA, 2004
18. Frisch, M. J.; Pople, J. A.; Binkley, J. S. J Chem Phys 1984, 80, 3265.
19. Simon, S.; Duran, M.; Dannenberg, J. J. J Chem Phys 1996, 105, 11024.
20. Boys, S. F.; Bernardi, F. Mol Phys 2002, 100, 65.
21. Grant, J. A.; Pickup, B. T.; Nicholls, A. J Comput Chem 2001, 22, 608.
22. Richards, F. M. Annu Rev Biophys Bioeng 1977, 6, 151.
23. Bondi, A. J Phys Chem 1964, 68, 441.
24. Singh, U. C.; Kollman, P. A. J Comput Chem 1984, 5, 129.
25. Anisimov, V. M.; Lamoureux, G.; Vorobyov, I. V.; Huang, N.; Roux, B.; MacKerell, A. D. J Chem Theory Comput 2005, 1, 153.
26. Elking, D.; Darden, T.; Woods, R. J. J Comput Chem 2007, 28, 1261.
27. Connolly, M. L. Science 1983, 221, 709.
28. Mobley, D. L.; Dumont, E.; Chodera, J. D.; Dill, K. A. J Phys Chem B 2007, 111, 2242.
29. Mobley, D. L.; Graves, A. P.; Chodera, J. D.; Shoichet, B. K.; Dill, K. A. Biophys J 2007, 368A.
30. Williams, D. E.; Abraha, A. J Comput Chem 1999, 20, 579.
31. Williams, D. E. J Comput Chem 1994, 15, 719.
32. Lopes, P. E. M.; Lamoureux, G.; Roux, B.; MacKerell, A. D. J Phys Chem B 2007, 111, 2873.
33. Kaminski, G. A.; Stern, H. A.; Berne, B. J.; Friesner, R. A.; Cao, Y. X. X.; Murphy, R. B.; Zhou, R. H.; Halgren, T. A. J Comput Chem 2002, 23, 1515.
34. Anisimov, V. M.; Vorobyov, I. V.; Lamoureux, G.; Noskov, S.; Roux, B.; MacKerell, A. D. Biophys J 2004, 86, 415A.
35. Stern, H. A.; Kaminski, G. A.; Banks, J. L.; Zhou, R. H.; Berne, B. J.; Friesner, R. A. J Phys Chem B 1999, 103, 4730.
36. Jorgensen, W. L.; Severance, D. L. J Am Chem Soc 1990, 112, 4768.

37. Caldwell, J. W.; Kollman, P. A. J Am Chem Soc 1995, 117, 4177.
38. Tsuzuki, S.; Yoshida, M.; Uchimaru, T.; Mikami, M. J Phys Chem A 2001, 105, 769.
39. Gallivan, J. P.; Dougherty, D. A. Proc Natl Acad Sci USA 1999, 96, 9459.
40. Roux, B. Chem Phys Lett 1993, 212, 231.
41. Ma, J. C.; Dougherty, D. A. Chem Rev 1997, 97, 1303.
42. Weiner, S. J.; Kollman, P. A.; Case, D. A.; Singh, U. C.; Ghio, C.; Alagona, G.; Profeta, S.; Weiner, P. J Am Chem Soc 1984, 106, 765.
43. Cornell, W. D.; Cieplak, P.; Bayly, C. I.; Gould, I. R.; Merz, K. M.; Ferguson, D. M.; Spellmeyer, D. C.; Fox, T.; Caldwell, J. W.; Kollman, P. A. J Am Chem Soc 1995, 117, 5179.
44. Guo, H.; Gresh, N.; Roques, B. P.; Salahub, D. R. J Phys Chem B 2000, 104, 9746.
45. Guo, H.; Salahub, D. R. Angew Chem Int Edit 1998, 37, 2985.
46. Chen, Y. F.; Dannenberg, J. J. J Am Chem Soc 2006, 128, 8100.
47. Harder, E.; Kim, B. C.; Friesner, R. A.; Berne, B. J. J Chem Theory Comput 2005, 1, 169.
48. Schropp, B.; Tavan, P. J Phys Chem B 2008, 112, 6233.
49. Luo, R.; David, L.; Gilson, M. K. J Comput Chem 2002, 23, 1244.
50. Prabhu, N. V.; Zhu, P. J.; Sharp, K. A. J Comput Chem 2004, 25, 2049.
51. Im, W.; Beglov, D.; Roux, B. Comput Phys Commun 1998, 111, 59.
52. Lu, Q.; Luo, R. J Chem Phys 2003, 119, 11035.